Geocell reinforced sand beds: Liquefaction resistance evaluation

P. Krishnaraj
Hamburg University of Technology, Hamburg, Germany, prerana.krishnaraj@tuhh.de

G.M. Latha
Indian Institute of Science, Bangalore, India, madhavi@iisc.ac.in

J. Grabe
Hamburg University of Technology, Hamburg, Germany, grabe@tuhh.de

ABSTRACT: This study investigates the impact of the geocell reinforcement on the liquefaction response of sand beds through experimental and numerical modeling. The experimental studies on sand beds were conducted through 1*g* shaking table model tests considering a scaling factor of 1:10. In case of reinforced sand beds, a 3D printed geocell layer of height 0.05 m was placed at a depth of 0.04 m from the surface. The results indicated that the geocell reinforcement has a beneficial effect on the liquefaction resistance of sand, with geocell reinforced sand beds exhibiting higher liquefaction resistance than unreinforced sand beds. The effectiveness of geocell reinforcement in enhancing liquefaction resistance increased at higher input accelerations, with inclusion of geocell reinforcement increasing the number of cycles required for liquefaction by 70% and 120%, for input acceleration value of 0.12*g* and 0.2*g*, respectively. The presence of geocell reinforcement not only impeded the pore water pressure buildup but also aided in reduction of acceleration developed in the sand bed. The numerical modelling was carried out using FLAC3D to gain insights into the field-scale behavior of sand beds. Through numerical study, the effects of various parameters such as depth of placement of the geocell layer, aspect ratio of the geocell, stiffness of the geocell, relative density of the sand and input acceleration on the efficacy of the geocell reinforcement in increasing the liquefaction resistance is analysed. Overall, the study yielded encouraging results, showcasing a higher liquefaction resistance of geocell reinforced sand beds in comparison to unreinforced sand beds.

1 INTRODUCTION

The widespread implementation of geocell reinforcement as ground improvement techniques makes it important to understand the liquefaction susceptibility of the geocell reinforced soils. Most of the soils reinforced with geocell fall to granular soils category, which when saturated are susceptible to liquefaction. Liquefaction is a phenomenon closely associated with saturated soil, where a loose saturated soil when loaded under undrained condition loses their shear strength due to the pore water pressure development and starts to flow like fluid (Dobry and Abdoun, 2017; Lashkari et al., 2017). This loss of shear strength causes significant damages to the structures or roads built on such soils. Hence, it is very important to analyse the liquefaction behaviour of the reinforced soils for accurate designing.

Due to the wide applicability of geosynthetics owing to their cost-effectiveness, rapid installation, and sustainability, large number of studies on the liquefaction resistance of the geosynthetic reinforced soils were carried out at laboratory element scale (Krishnaswamy and Isaac, 1994; Vercueil et al., 1997; Moayed and Alibolandi, 2018; Su et al., 2022; Noorzad and Amini, 2014; Rasouli and Fatahi, 2022) and model scale (Maheshwari et al., 2012; Mittal and Chauhan, 2013; Bahadori et al., 2020) level. Though extensive work has been carried out on the liquefaction response of the soils reinforced with planar or fiber geosynthetics, the same cannot be quoted on the soils reinforced with geocells. To address this knowledge gap, the current study carried out experimental shaking table tests and numerical modelling to simulate the liquefaction response of the saturated sand beds reinforced with geocells. The study provided preliminary insights into the role of the geocell reinforcement in the liquefaction resistance of sand beds.

2 MATERIALS AND METHODOLOGY

2.1 Materials used

2.1.1 Sand

The experimental studies were carried out on sand from Cauvery river basin in India. The particle size distribution curve for the sand is shown in Figure 1. Preliminary analysis on sand showed that it belongs to poorly graded (SP) category based on unified soil classification system (USCS), as per ASTM D2487. The consolidated undrained triaxial tests carried out in the present study showed that the sand demonstrated a cohesive strength and effective friction angle of 0 kPa and 34.8°, respectively.

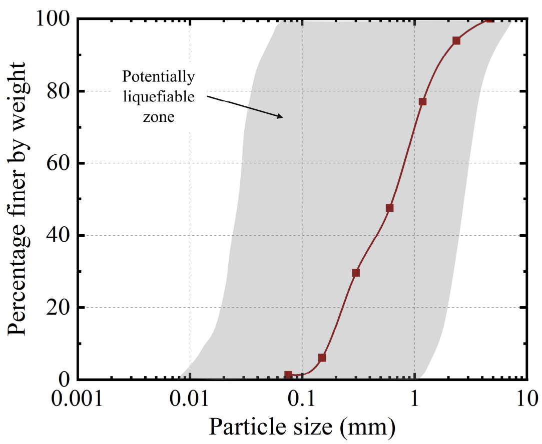

Figure 1. Particle size distribution plot for sand.

2.1.2 Reinforcement

Indigeneously fabricated 3D printed low strength geocell mats were used to reinforce the saturated sand beds. The fabrication of the geocell was carried out in accordance with the scaling requirements of 1*g* model tests. An in-detail description of the 3D printed geocell fabrication is available in Venkateswarlu et al. (2023) and Krishnaraj and Latha (2024). The physical dimension and the tensile strength properties of the geocell reinforcement were obtained corresponding to the scaling factor of 10. In the current study, the geocell mats with pockets of effective diameter 50 mm and height 50 mm and an ultimate tensile strength of 3.32 kN/m were used. Figure 2 gives the image of the 3D printed geocell mat used in the shaking table studies.

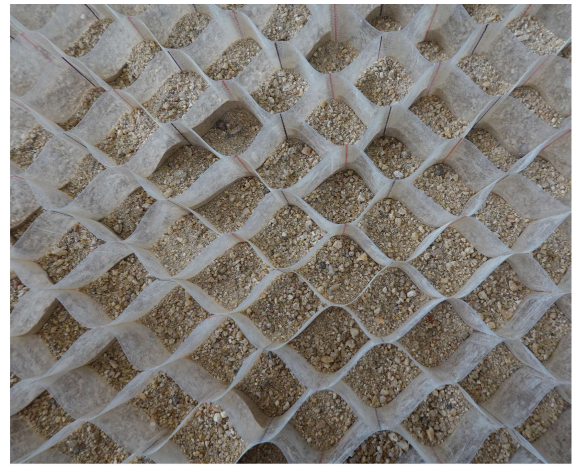

Figure 2. 3D printed geocell mat.

2.2 Testing method

The liquefaction resistance of the geocell reinforced sand beds was analysed using 1*g* shaking table testing. The testing was carried out on sand beds of height 0.6 m and area 1.2 m × 0.5 m, contained in a transparent Perspex box. In case of geocell reinforced sand beds, the geocell reinforcement was placed at a depth of 0.04 m from the surface. A linear scaling factor of 10 was considered in this study, which corresponds to a field scale sand bed of dimension 12 m × 5 m × 6 m. The shaking table apparatus used in the study facilitates uni-directional horizontal shaking. The horizontal shaking is displacement controlled, where a displacement corresponding to an acceleration of particular amplitude and frequency is applied to base of the Perspex box. A detailed description on the shaking table apparatus can be found in Krishnaraj et al. (2023). However, it should be noted that a Perspex box is used instead of laminar shear box to maintain the water tightness of the system (a criteria necessary for liquefaction studies).

The sand beds in the current study were maintained at a relative density of 30% (representing a loose state). The wet pluviation technique was implemented to prepare the sand bed, as this technique closely represents the natural deposition process and also results in a homogeneous sand bed (Vaid and Negussey, 1988). During the preparation of the reinforced sand beds, the pluviation is halted when the depth of placement of the geocell reinforcement was reached and the geocell reinforcement was placed and pluviation is continued until the sand bed of the required height was achieved. To analyse the performance of the sand beds under dynamic loading, pore water pressure and acceleration amplification in the sand bed were determined. The miniature pore water pressure transducers with a pressure range of 0 to 20 kPa and accelerometers with a measuring range of ±3g were placed along the center line of the sand bed at depths 100 mm, 300 mm and 500 mm from the surface. Figure 3 shows a schematic representation of the geocell reinforced sand bed, with emphasis on the measurement locations.

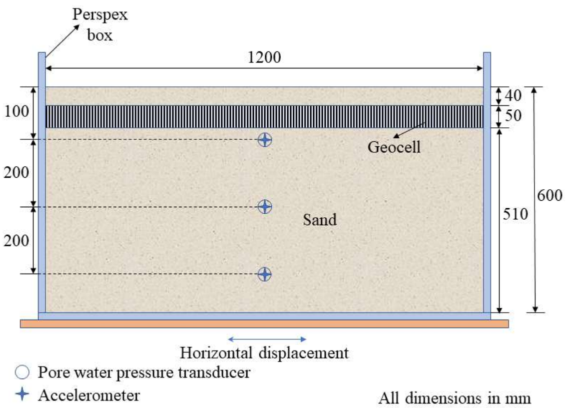

Figure 3. A schematic representation of the layout of the geocell reinforced sand beds.

3 OUTCOMES FROM THE EXPERIMENTAL STUDY

The performance of the unreinforced and geocell reinforced sand beds were compared at different values of input accelerations. A thorough analysis in terms of pore water pressure development and the acceleration amplification in sand beds was carried out. The sand beds were subjected to sinusoidal base accelerations of amplitude 0.12g, 0.15g and 0.2g, at a frequency of 1 Hz.

3.1 Analysis on the basis of pore water pressure

The pore water pressure readings from the transducers placed at a depth of 100 mm from the surface is reported here. Figure 4 gives the progression of the pore water pressure (r_u) with number of cycles (N_c) for both unreinforced and geocell reinforced sand beds. Here the value of r_u was calculated as the ratio of the excess pore water pressure developed to the initial effective vertical stress. The onset of the liquefaction corresponds to the point where the value of r_u becomes equal to 1.

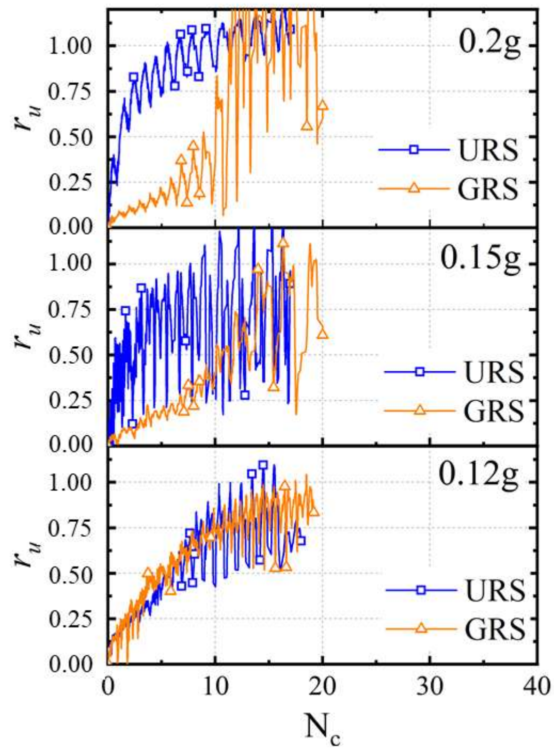

Figure 4. The variation of the pore water pressure ratio (r_u) with number of loading cycle (N_c) for unreinforced and geocell reinforced sand beds for input acceleration values of 0.12g, 0.15g and 0.2g.

The progression of the pore water ratio with loading shows that the dynamic loading led to an increase in the pore water pressure ratio in all sand beds. However, the rate of increase in r_u was found to increase with an increase in amplitude of acceleration. It should be noted that both unreinforced and geocell reinforced sand beds liquefied for all the input acceleration values considered. However, the loading cycle at which the liquefaction onset was observed was significantly influenced by the reinforcement, with number of loading cycles required for the reinforced sand beds to liquefy was evidently higher than the unreinforced sand beds. For the input acceleration value of 0.12g, the unreinforced sand bed liquefied at cycle number 10, in comparison to which the geocell reinforced sand bed required 17 cycles to liquefy, demonstrating a higher liquefaction resistance.

Irrespective of the reinforcement condition, with the increase in the magnitude of the input acceleration, a noticeable reduction in the liquefaction resistance of the sand beds was observed. For increase in input acceleration value from 0.12g to 0.2g. the number of loading cycles required for the unreinforced sand beds to liquefy reduced from 10 to 5 cycles. Following a similar trend, the loading cycles required for the onset of the liquefaction reduced from 17 to 12 cycles for reinforced sand beds. This indicates that the presence of the geocell reinforcement enhanced the liquefaction resistance (in terms of number of loading cycles) by 70% and 120%, for the input acceleration values of 0.12*g* and 0.2*g*, respectively.

3.2 Analysis on the basis of the acceleration developed in the sand bed

The acceleration readings from the accelerometers for the unreinforced sand bed for the input acceleration value of 0.12*g* was analysed. With the progression in the loading, the amplitude of the acceleration increases, reaching its maximum at the onset of the liquefaction, followed by a reduction in the amplitude, indicating soil softening and stiffness degradation.

As the acceleration amplitude reaches a maximum at the onset of the liquefaction, a comparison in the performance of the unreinforced and geocell reinforced sand beds was carried out by a dimensionless parameter called '*Acceleration Amplification Factor* (*AAF*)'. *AAF* is calculated as the ratio of the maximum acceleration amplitude recorded at a particular depth in the sand bed to the base input acceleration. At a depth of 100 mm, the value of *AAF* was found to be 1.83 and 1.5 for unreinforced and geocell reinforced sand beds, indicating a better performance reinforced sand beds.

4 NUMERICAL ANALYSIS

To understand and analyse the liquefaction response of the geocell reinforced sand beds at field scale, numerical modelling was carried out using FLAC3D (Fast Lagrangian Analysis of Continua in 3 Dimensions). A scaling factor of 10 was considered in the analysis, which resulted in a sand bed of dimension 12 m (Length) × 5 m (Width) × 6 m (Height). The numerical model was validated against the experimental data. The validated model was further used to carry out parametric studies to study the effects of the geocell aspect ratio, geocell placement depth, geocell stiffness, the relative density of the sand and the amplitude of input acceleration on the liquefaction response of the sand beds.

The variation of the pore water pressure ratio at different depths show that the influence of the geocell reinforcement reduces as the depth of the point under consideration increases. This shows that for every combination of loading and in-situ conditions, there exists a particular depth within which the presence of the geocell reinforcement completely mitigates the occurrence of the liquefaction. This depth is termed as "Depth of improvement". The value of r_u is less than 1 for any point within the depth of improvement.

4.1 Effect of geocell aspect ratio and depth of placement

This section describes the combined effect of the geocell aspect ratio and geocell placement depth on the depth of improvement. To analyse the combined effect of both these parameters, a dimensionless quantity, called *Placement Factor* (*PF*) is calculated as $((a \times u) / (h + u))$, where a is the geocell aspect ratio, u is the depth of placement of the geocell and h is the height of the geocell layer. The variation of the normalized depth of improvement for different values of *PF* is given in Figure 5. With the increase in the value of *PF*, the depth of improvement increases. For a particular loading and in-situ conditions, there exists a value of *PF* beyond which the liquefaction is mitigated throughout the depth of interest. This highlights the importance of the selection of appropriate placement condition and geocell dimensions for a particular liquefaction mitigation application.

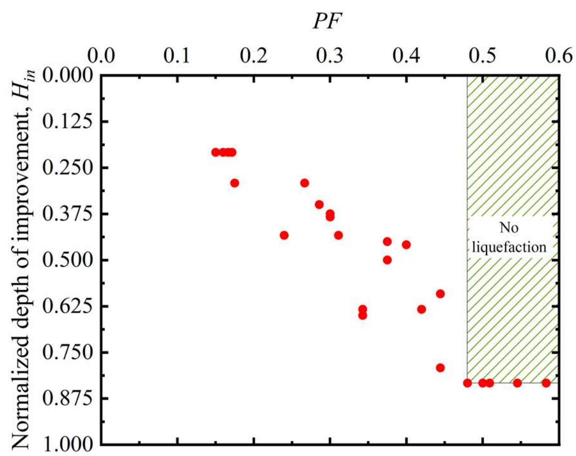

Figure 5. Variation of the normalized depth of improvement with the Placement Factor (PF).

4.2 Effect of geocell stiffness

Not only the placement parameters, the stiffness of the geocell also plays an important role in the reduction of the pore water pressure developed during the loading. To analyse this, a wide range of geocell stiffness varying from 50 MPa to 600 MPa were considered for the analysis. The variation of the normalised depth of improvement with the geocell stiffness is plotted in Figure 6. The plot shows that, with an increase in the geocell stiffness, the depth of influence of geocell on the pore water pressure development increases. For the same placement and loading conditions, the sands reinforced with geocells of higher stiffness demonstrate a higher liquefaction resistance.

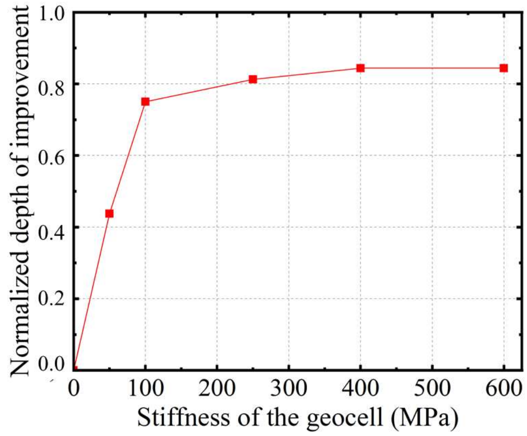

Figure 6. Effect of geocell stiffness on depth of improvement.

4.3 Effect of relative density of infill sand

The infill sand in the geocell pockets are most often densified. However, all the previous analysis in this study were carried out considering a relative density of 30% throughout the sand bed. To analyse the effect of the infill relative density, two different infill relative densities of 30% and 70% was considered. The plot of the maximum pore water pressure ratio ($r_{u,max}$) with depth (Figure 7) shows that the increase in the infill relative density further hampers the development of the pore water pressure in the sand beds.

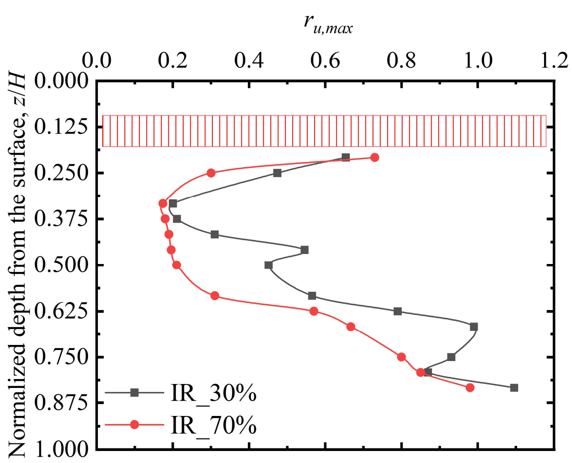

Figure 7. Maximum pore water pressure ratio ($r_{u,max}$) recorded at different depths for geocell reinforced sand beds with infill relative densities of 30% and 70%.

4.4 Effect of input acceleration

To analyse the effect of input acceleration on the depth of improvement, simulations were carried out for acceleration ranging from 0.12g to 0.4g. With the increase in the input acceleration value, the depth of influence of the geocell reinforcement evidently decreased, as observed from Figure 8. This indicates that, for the region with higher seismicity, the liquefaction resistance can be increased by selecting geocells with adequate placement factor *PF* or higher stiffness.

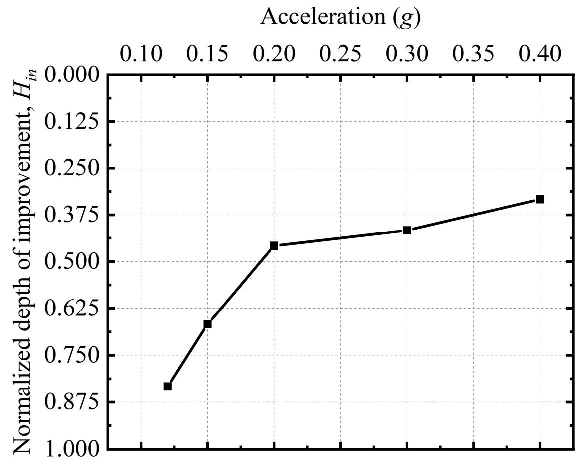

Figure 8. Effect of input acceleration on the depth of improvement.

5 CONCLUSIONS

The presence of geocell reinforcement significantly impacted the liquefaction response of the sand beds, as demonstrated by both experimental and numerical modelling results. The following conclusions can be drawn from the present study:

- The experimental shaking table tests showed that the presence of the geocell reinforcement delayed the onset of the liquefaction with number of cycles required to liquefy increased by 70% and 120% for the input acceleration values of 0.12g and 0.2g, respectively.
- The geocell reinforced sand beds also showed a lower acceleration amplification as compared to unreinforced sand beds.
- The numerical analysis showed the presence of depth of improvement beneath the geocell layer, beyond which the influence of the geocell reinforced is negligible. This depth of improvement was found to depend on depth of placement of the geocell layer, aspect ratio of the geocell, stiffness of the geocell, infill sand relative density and the input acceleration.

REFERENCES

ASTM D2487-17 (2017) Standard practice for classification of soils for engineering purposes (Unified Soil Classification System), Conshohocken, PA, USA.

Bahadori, H., Motamedi, H., Hasheminezhad, A., & Motamed, R. (2020). Shaking table tests on shallow foundations over geocomposite and geogrid-reinforced liquefiable soils. *Soil Dynamics and Earthquake Engineering*, *128*, 105896. https://doi.org/10.1016/j.soildyn.2019.105896

Dobry, R., & Abdoun, T. (2017). Recent findings on liquefaction triggering in clean and silty sands during earthquakes. *Journal of geotechnical and geoenvironmental engineering*, *143*(10), 04017077. https://doi.org/10.1061/(ASCE)GT.1943-5606.0001778

Krishnaraj, P., & Latha, G. M. (2024). Additive Manufacturing of Geocells: Technological, Mechanical and Micro-Structural Aspects. *International Journal of Geosynthetics and Ground Engineering*, *10*(3), 32. https://doi.org/10.1007/s40891-024-00554-2

Krishnaraj, P., Manju, G.S. and Latha, G.M., 2023. Physical and numerical shaking table studies on geocell-reinforced retaining walls. *International Journal of Geosynthetics and Ground Engineering*, *9*(5), p.62. https://doi.org/10.1007/s40891-023-00482-7

Krishnaswamy, N. R., & Isaac, N. T. (1994). Liquefaction potential of reinforced sand. *Geotextiles and Geomembranes*, *13*(1), 23-41. https://doi.org/10.1016/0266-1144(94)90055-8

Lashkari, A., Karimi, A., Fakharian, K., & Kaviani-Hamedani, F. (2017). Prediction of undrained behavior of isotropically and anisotropically consolidated Firoozkuh sand: instability and flow liquefaction. *International Journal of Geomechanics*, *17*(10), 04017083. https://doi.org/10.1061/(ASCE)GM.1943-5622.0000958

Maheshwari, B. K., Singh, H. P., & Saran, S. (2012). Effects of reinforcement on liquefaction resistance of Solani sand. *Journal of Geotechnical and Geoenvironmental Engineering*, *138*(7), 831-840. https://doi.org/10.1061/(ASCE)GT.1943-5606.0000645

Mittal, S., & Chauhan, R. (2013). Liquefaction behavior of reinforced saturated sand under dynamic conditions. *International Journal of Geotechnical Engineering*, *7*(1), 109-114. https://doi.org/10.1179/1938636212Z.0000000008

Moayed, R. Z., & Alibolandi, M. (2018). Effect of geotextile reinforcement on cyclic undrained behavior of sand. *Soil Dynamics and Earthquake Engineering*, *104*, 395-402. https://doi.org/10.1016/j.soildyn.2017.11.013

Noorzad, R., & Amini, P. F. (2014). Liquefaction resistance of Babolsar sand reinforced with randomly distributed fibers under cyclic loading. *Soil Dynamics and Earthquake Engineering*, *66*, 281-292. https://doi.org/10.1016/j.soildyn.2014.07.011

Rasouli, H., & Fatahi, B. (2022). Liquefaction and post-liquefaction resistance of sand reinforced with recycled geofibre. *Geotextiles and Geomembranes*, *50*(1), 69-81. https://doi.org/10.1016/j.geotexmem.2021.09.002

Su, L., Zhou, L., Zhang, X., & Ling, X. (2022). Experimental and numerical modeling on liquefaction resistance of geotextile reinforced sand. *Soil Dynamics and Earthquake Engineering*, *159*, 107345. https://doi.org/10.1016/j.soildyn.2022.107345

Vaid, Y.P. and Negussey, D. (1988). Preparation of reconstituted sand specimens. Advanced Triaxial Testing of Soil and Rock, ASTM STP 977, pp. 405-417. https://doi.org/10.1520/STP29090S.

Venkateswarlu, H., Krishnaraj, P., & Latha, G. M. (2023). Three-dimensionally printed polypropylene sheets: insights on mechanical and interface shear behavior. *Journal of Materials in Civil Engineering*, *35*(9), 04023284. https://doi.org/10.1061/JMCEE7.MTENG-15089

Vercueil, D., Billet, P., & Cordary, D. (1997). Study of the liquefaction resistance of a saturated sand reinforced with geosynthetics. *Soil Dynamics and Earthquake Engineering*, *16*(7-8), 417-425. https://doi.org/10.1016/S0267-7261(97)00018-3